Construction of an Aptamer–SiRNA Chimera-Modified Tissue-Engineered Blood Vessel for Cell-Type-Specific Capture and Delivery

Wen Chen,[†] Wen Zeng,[†] Jiansen Sun, Mingcan Yang, Li Li, Jingting Zhou, Yangxiao Wu, Jun Sun, Ge Liu, Rui Tang, Ju Tan, and Chuhong Zhu*

Department of Anatomy, National & Regional Engineering Laboratory of Tissue Engineering, Key Lab for Biomechanics and Tissue Engineering of Chongqing, Third Military Medical University, Chongqing 400038, China. [†]W. Chen and W. Zeng contributed equally to this work.

ABSTRACT The application of tissue-engineered blood vessels (TEBVs) is the main developmental direction of vascular replacement therapy. Due to few and/or dysfunctional endothelial progenitor cells (EPCs), it is difficult to successfully construct EPC capture TEBVs in diabetes. RNA has a potential application in cell protection and diabetes treatment, but poor specificity and low efficiency of RNA transfection *in vivo* limit the application of RNA. On the basis of an acellular vascular matrix, we propose an aptamer–siRNA chimera-modified TEBV that can maintain a satisfactory patency in diabetes. This TEBV consists of two parts, CD133-adenosine kinase (ADK) chimeras and a TEBV scaffold. Our results showed that CD133-ADK chimeras could selectively capture the CD133-positive cells *in vivo*, and then captured cells can internalize the bound chimeras to achieve RNA self-transfection. Subsequently, CD133-ADK chimeras were cut into ADK siRNA by a dicer, resulting in depletion of ADK. An ADK-deficient cell may act as a bioreactor that sustainably releases adenosine. To reduce nonspecific RNA transfection, we increased the proportion of $HAuCl_4$ during the material preparation, through which the transfection capacity of polyethylenimine (PEI)/polyethylene glycol (PEG)-capped gold nanoparticles (PEI/PEG-AuNPs) was significantly decreased and the ability of TEBV to resist tensile and liquid shear stress was greatly enhanced. PEG and 2′-*O*-methyl modification was used to enhance the *in vivo* stability of RNA chimeras. At day 30 postgrafting, the patency rate of CD133-ADK chimera-modified TEBVs reached 90% in diabetic rats and good endothelialization was observed.

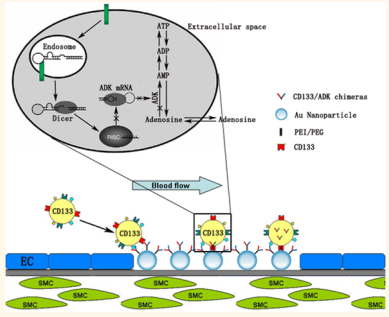

KEYWORDS: diabetes mellitus · CD133 · adenosine kinase · tissue-engineered blood vessels · aptamer–siRNA chimeras

Diabetes mellitus is a worldwide chronic metabolic disease that results in tremendous economic and social burdens.[1] The most common complications of diabetes are diabetic angiopathy and diabetic nephropathy; the former mostly occurs in the cardiac and brain vascular system, leading to a high risk of death of diabetic patients, while the latter is the leading cause for hemodialysis in adults in developing countries. Diabetic angiopathy requires replacement therapy to treat lesioned vessels, and diabetic nephropathy requires hemodialysis treatment during which punctures are performed repeatedly on the vascular bypass grafts. The application of tissue-engineered blood vessels (TEBVs) has been generally recognized as the main developmental direction of vascular replacement therapy.[2] Currently, many kinds of TEBVs have been used for vascular replacement or hemodialysis access and achieved good results under certain conditions.[3−5] However, patients who require vascular replacement therapy always have primary disease such as diabetes mellitus or other cardiovascular diseases. Until now, no successful construction of TEBVs in the replacement of end-stage diabetic vessels has been reported.

To minimize invasive procedures in patients by avoiding autologous cell harvesting, bioengineered grafts without endothelial cells is a major point of research in the future.[6,7] Endothelial progenitor cells (EPCs) are the precursor cells of endothelial cells.[8] Through coating specific molecules and antibodies on the inner surface of an

* Address correspondence to (C. Zhu) zhuch99@yahoo.com.

Received for review February 23, 2015 and accepted June 7, 2015.

Published online June 08, 2015
10.1021/acsnano.5b01203

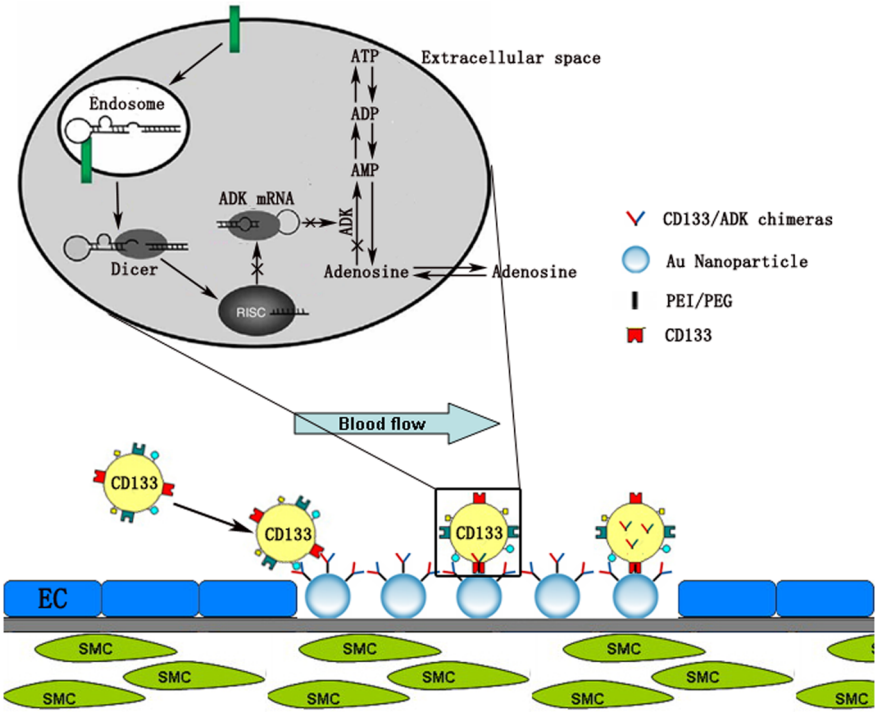

Scheme 1. Construction of an aptamer−siRNA chimera-modified TEBV for cell-type-specific capture and delivery. CD133-ADK chimera-modified TEBV consisted of two parts, CD133-ADK chimeras and a TEBV scaffold. PEI/PEG-AuNPs act as bridges to connect the TEBV scaffolds and CD133-ADK chimeras. CD133-ADK chimeras could selectively capture the CD133-positive cells in the blood, and the captured cells internalized the bound chimeras to achieve RNA self-transfection. Subsequently, CD133-ADK chimeras were released from the endosome and cut into ADK siRNA by a dicer. Then the RNA-induced silencing complex (RISC) that contained an ADK siRNA strand mediated targeted mRNA degradation, further resulting in depletion of ADK. ADK is a nucleoside kinase that catalyzes adenosine to form ATP, and ADK inhibition helps to maintain cellular energy metabolism to protect seed cells from hyperglycemia-induced damage in diabetes. Furthermore, an ADK-deficient cell may act as a bioreactor that sustainably releases adenosine, leading to the significant optimization of the microenvironment and promotion of angiogenesis.

acellular vascular matrix or other materials, researchers have constructed TEBVs that can *in vivo* capture EPCs and achieve satisfactory durable patency.[9,10] The research progress regarding the development of intravascular stents may provide insights and knowledge useful for the construction of TEBVs in diabetes mellitus. EPC capture stents could enhance rapid endothelialization in animal models, but they may fail in clinical application because patients with diabetes or other cardiovascular disease always have dysfunctional and/or few EPCs. This can be ameliorated by enhancing the EPC number and survival in patients.[11,12] Therefore, it might be applicable to improve the function of homed stem cells and increase the number of EPCs in blood circulation *via* gene regulation to promote the patency of grafted TEBVs under diabetic conditions.

Adenosine kinase (ADK) is a nucleoside kinase that catalyzes adenosine to form adenosine 5-triphosphate (ATP).[13] Studies have shown that ADK upregulation accelerates cellular damage and death under ischemic conditions, and ADK inhibition helps to maintain cellular energy metabolism to fight against disease hazards.[14,15] Furthermore, ADK-deficient cells can sustainably release adenosine, which improves the local microenvironment through its functions such as those in inflammatory regulation, cell protection, and pro-angiogenesis.[13,16] All of the above support the possibility of ADK as a functional target of stem cells under diabetic conditions. CD133 is a highly specific surface marker of EPCs, and CD133-positive cells can promote the formation of blood vessels through the paracrine functions.[17]

Here we prepared an aptamer−siRNA chimera-modified TEBV for cell-type-specific capture and delivery. The strategy that we propose has many advantages (Scheme 1): First, the CD133-ADK chimeras can specifically capture and self-transfect into target cells, a feature that is different from the traditional RNA delivery method used in the construction of tissue-engineering materials. Second, using ADK as a target, CD133-ADK chimeras can not only reverse the impaired stem cell function and protect cells but also turn cells into "bioreactors" that constantly produce adenosine to further significantly optimize the microenvironment and promote the mobilization of EPCs. Third, the increase in the proportion of Au in PEI/PEG-AuNPs decreases nonspecific RNA transfection and improves the antishearing force and tensile strength of TEBVs. In addition, PEG and 2′-*O*-methyl (2′-OMe) modification were used to enhance the *in vivo* stability of RNA chimeras.[18] Finally, TEBV scaffolds and RNA are

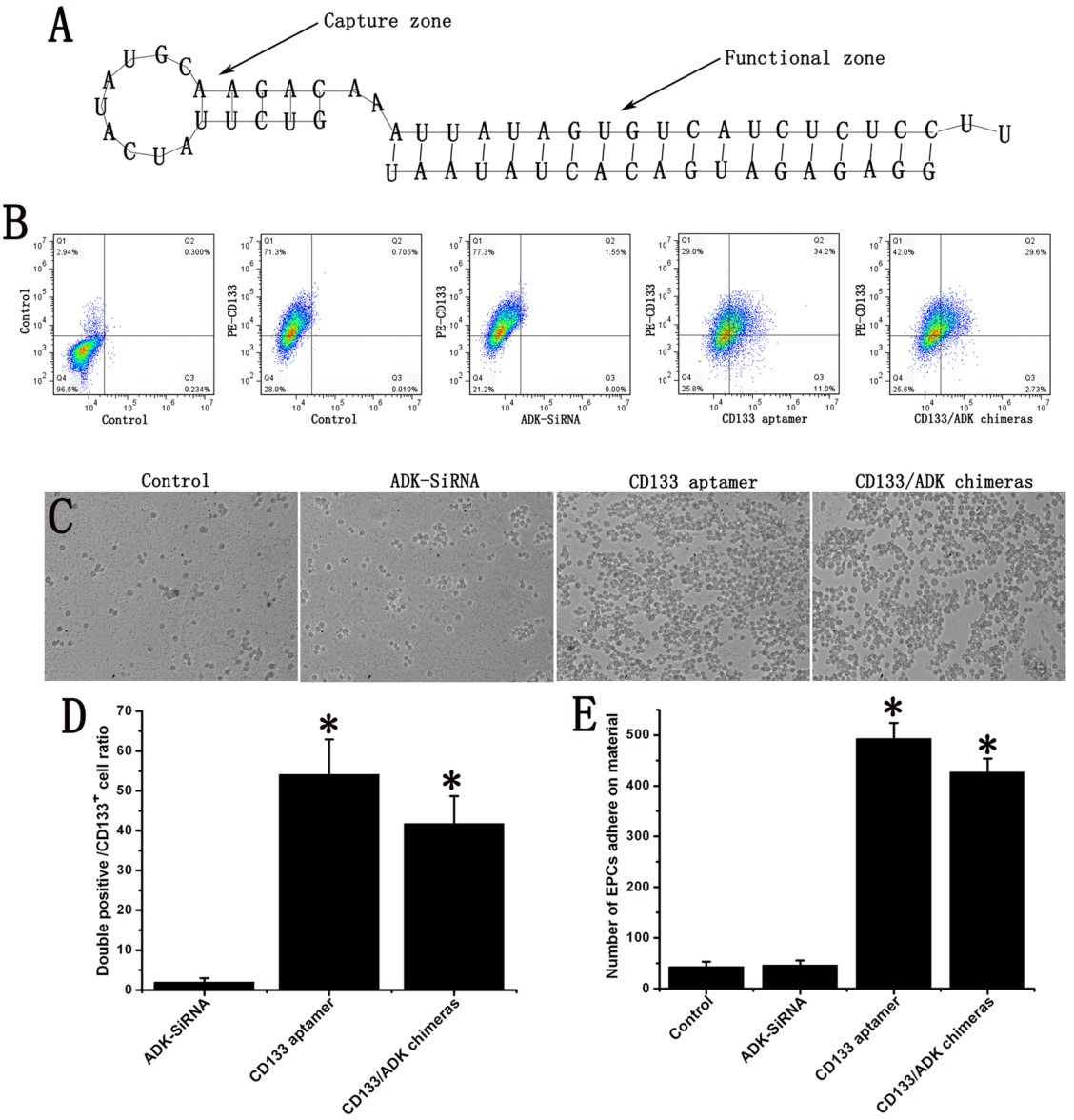

Figure 1. CD133-ADK chimeras could specifically bind to CD133-positive cells. (A) Predicted secondary structure for the CD133-ADK chimeras. (B) After selective cultivation, the cells were incubated with FAM-RNA, FAM-CD133 aptamer, and FAM-CD133-ADK chimeras in the presence of PE-CD133 antibody. Proportion of bound cells was assessed by flow cytometry. (C) Parallel-plate flow chamber was used to detect the effect of CD133-ADK chimeras on capturing flowing cells. (D) Flow cytometry showed CD133 aptamer and CD133-ADK chimeras could specifically bind to CD133-positive cells. (E) CD133 aptamer and CD133-ADK chimeras could effectively capture flowing CD133-positive cells. *$p < 0.05$ ($n = 6$) *versus* ADK-SiRNA. Values are mean ± SD.

separately stored, and they are freshly assembled prior to grafting, allowing the maximum preservation of RNA bioactivity; this method is also suitable for the application of other materials.

RESULTS AND DISCUSSION

In this paper, we first designed CD133-ADK chimeras. The predicted secondary structure of CD133-ADK chimeras is demonstrated in Figure 1A. This chimera was divided into CD133 aptamer and ADK siRNA. CD133 aptamer was the capture zone, which could specifically capture CD133-positive cells. ADK siRNA was the functional zone, which suppressed high-glucose-induced cell apoptosis and promoted the paracrine of angiogenesis factors (Figures S1 and S2). The increased vascular endothelial growth factor (VEGF), stromal cell-derived factor-1 (SDF-1), and interleukin-8 (IL-8) from CD133-ADK chimera-bound cells promoted endothelial cell migration and the healing of scratches (Figures S3 and S4). Moreover, SDF-1 and VEGF, also known as stem/progenitor cell mobilization-associated molecules, could promote EPC mobilization from bone marrow, further increasing the number of EPCs in the blood.[19,20]

To detect the ability of CD133-ADK chimeras to bind CD133-positive cells, we used CD133-PE antibody as

the positive control. Flow cytometry demonstrated that approximately 71% of cultured cells were positive for CD133 after 5 day of selective culturing. ADK RNA did not specifically bind to CD133-positive cells. The CD133 aptamer bound to 53% of CD133-positive cells. CD133-ADK chimeras showed the ability to specifically bind to CD133-positive cells, with a binding ratio of approximately 41.6%, while nonspecifically bound cells accounted for 8% (Figure 1B). These results indicated that CD133-ADK chimeras could specifically recognize CD133-positive cells. To study the effect of CD133-ADK chimeras on intracellular ADK expression, we detected adenosine concentration in cell cultures. CD133-ADK chimera-bound CD133-positive cells could continuously release adenosine for 7 d, with a peak at the third day, and the peak level was approximately 6.47 times that of the control group (Figure S2a).

To investigate the CD133-positive-cell-capturing capability of CD133-ADK chimeras, we used a parallel plate flow chamber to simulate the inner surface of TEBVs. The results revealed that ADK siRNA did not capture the flowing CD133-positive cells. The CD133 aptamer could capture the flowing CD133-positive cells,as evidenced by the data that the number of cells adherent to the CD133 aptamer increased by 9.4 times compared with the control group. CD133-ADK chimeras could capture the flowing CD133-positive cells, and the number of adhered cells increased by 8.3 times compared with the control group (Figure 1C). To study the recruitment phenomenon, we transplanted CD133-ADK chimera or CD133 aptamer modified TEBVs *in vivo*. The CD133 immunofluorescence assay showed that at postgrafting day 1 the TEBVs in both the CD133-ADK chimera and CD133 aptamer group showed expression of CD133-positive cells on the inner wall. The patency rate of TEBVs was 40% in the siRNA control group, and few CD133-positive cells were observed in unobstructed TEBVs (Figure S5).

Polyethylenimine (PEI)/polyethylene glycol (PEG)-capped gold nanoparticles (PEI/PEG-AuNPs) act as bridges to connect the TEBV scaffolds and CD133-ADK chimeras. To detect the capability of nanoparticles to be transfected into CD133-negative cells, we selected vascular smooth muscle cells (SMCs) that were abundant in the carotid arterial wall and easily transfected by siRNA as transfection subjects. Flow cytometry revealed that PEI could achieve a smooth siRNA transfection into SMCs, while low-density PEI/PEG-AuNPs exhibited a stronger transfection capability and achieved a mean fluorescence intensity in SMCs 1.29 times higher than that in the PEI group. However, the increase in the Au concentration added during the preparation process greatly inhibited the transfection ability of PEI/PEG-AuNPs, leading to the average fluorescence intensity in SMCs being only 41% of that in the PEI group (Figure 2C).

There are high requirements for the stability of TEBVs, because transplanted TEBVs have to face fluid shear stresses of high intensities and an extremely complex microenvironment. After exposure to liquid shear stress for 48 h, FAM-modified siRNA in the college group hardly remained; a portion of FAM-modified siRNA remained in the PEI cross-linked group that was much less than that remaining in the PEI/PEG-AuNPs group. The increased concentration of Au added during the preparation process could remarkably increase the remaining FAM-modified siRNA, thus enhancing the ability of TEBVs to resist shear stress (Figure 2A and B).

The average maximum load and tensile strength of the vascular acellular scaffolds were only 0.12 N and 0.22 MPa, respectively, which could be increased by 3.92 and 3.91 times, respectively, through incubation and cross-linking with collagen. The cross-linking with PEI/PEG-AuNPs further enhanced the ability of TEBVs to resist tensile stress; compared with TEBVs incubated with only collagen, the average maximum load and tensile strength of high-density PEI/PEG-AuNP-modified TEBVs increased by 25.42% and 26.85%, respectively (Figure 2E).

We used vascular matrix material as the TEBV scaffolds. Hematoxylin and eosin (HE) staining showed that vascular acellular scaffolds contained only collagen, and the presence of the remaining cells was hardly noticeable. After incubation, collagen formed a smooth surface without any significant protrusions. After a further coating of high-density PEI/PEG-AuNPs, the nanoparticles of approximately 50−150 nm in diameter were evenly cross-linked on the collagen surface (Figure S6).

To study the effect of the CD133 aptamer and CD133-ADK chimera on TEBV patency, the TEBVs were transplanted into the rats not induced to be hyperglycemic. At postgrafting day 30, the patency rate of control siRNA-modified TEBV is only 10%. TEBVs in the CD133-ADK chimera group and CD133 aptamer group had a patency rate of 90% and 70% and had no significant intimal hyperplasia, respectively. These results showed that the CD133 aptamer could increase the TEBV patency rate through capturing EPCs in the blood. PEG and 2′-OMe modification effectively enhanced the *in vivo* stability of RNA (Figure S7).

Then TEBVs in each group were grafted into the common carotid artery of diabetic rats, followed by vascular anastomosis. Grafted TEBVs were removed at postgrafting day 7, 14, and 30. Micro-computed tomography (micro-CT) revealed that at postgrafting day 30 the TEBV graft on the right side in the rats of the CD133-ADK chimera group showed normal contrast enhancement and had similar lumen to the vessels at the opposite side and a trace of vessel grafting. By contrast, TEBVs in the siRNA control group and CD133 aptamer group did not show normal contrast

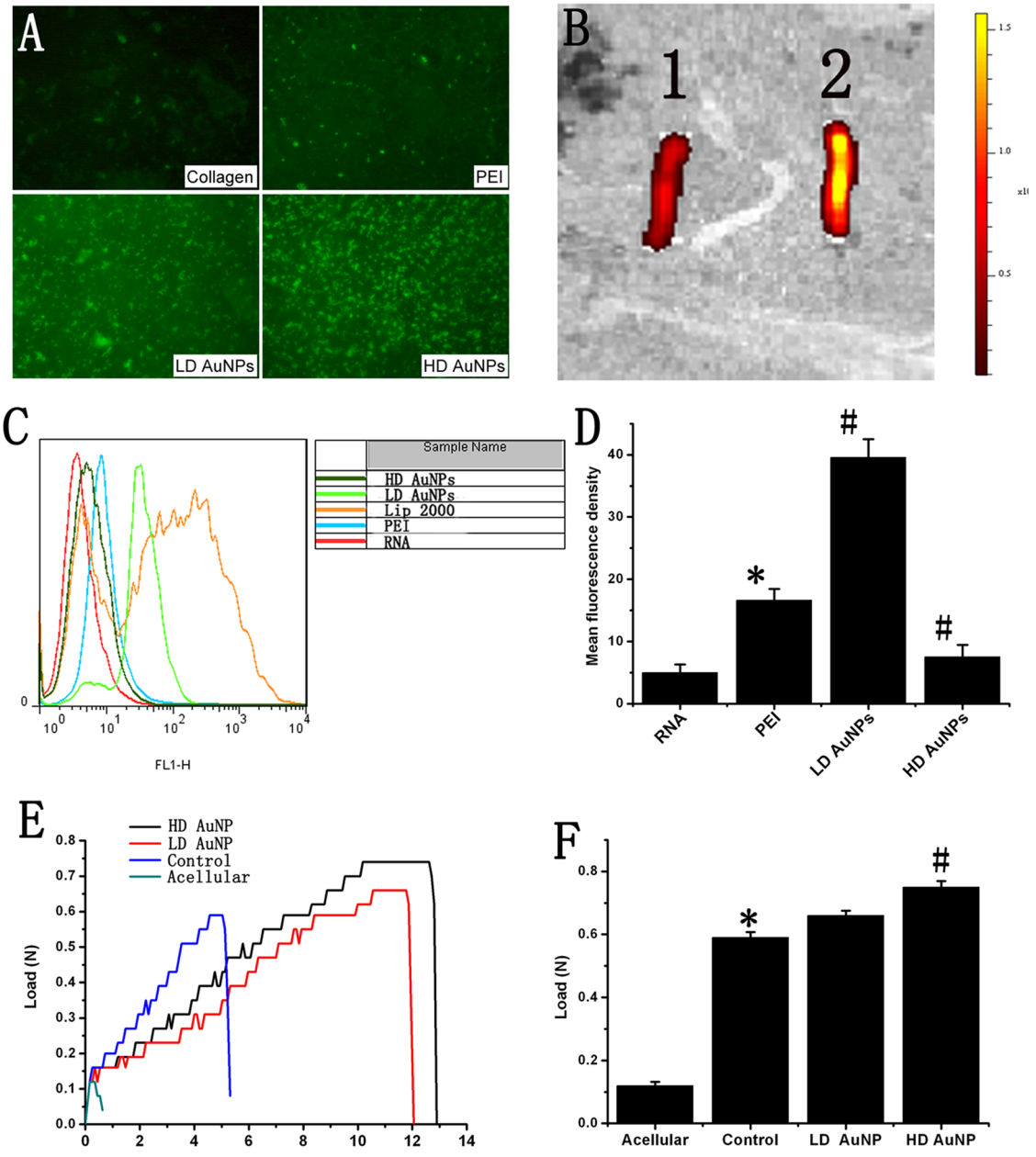

Figure 2. AuNPs enhanced antishearing force and tensile strength of TEBVs. (A) The collagen was cross-linked with PEI, low-density PEI/PEG-AuNPs (LD AuNPs), or high-density PEI/PEG-AuNPs (HD AuNPs) and then incubated with FAM-SiRNA for 15 min. Circulating pump drive PBS shear for 48 h and the fluorescence were determined. (B) The LD AuNPs and HD AuNPs were characterized on the interior surface of the TEBV, respectively, and then the prepared TEBVs were grafted onto the common carotid artery after incubating with FAM-CD133-ADK chimeras. The transplanted TEBVs were removed after 48 h, and the fluorescence intensity was determined by a fluorescence imaging detection system. (C) Vascular smooth muscle cells were used to detect the transfection capacity. The transfected cells were assessed by flow cytometry, and the results are presented as mean fluorescence intensity (MFI). (D) Compared with the PEI group, the MFI in the LD AuNP group increased by 129%. The MFI in the HD AuNP group decreased to 41% of that in the PEI group. *$p < 0.05$ ($n = 6$) *versus* RNA. $^{\#}p < 0.05$ ($n = 6$) *versus* PEI. (E) Computer-controlled electronic universal testing machine was used to detect the maximum load and tensile strength of the acellular vascular matrix, collagen control TEBV, LD AuNP modified TEBV, and HD AuNP modified TEBV. (F) AuNP-enhanced tensile strength of TEBV. *$p < 0.05$ ($n = 10$) *versus* acellular vascular matrix. $^{\#}p < 0.05$ ($n = 10$) *versus* collagen control TEBV. Values are mean ± SD.

enhancement, indicating occlusion of TEBVs (Figure 3E). HE staining results demonstrated that the siRNA control group had thrombosis-induced vascular occlusion at postgrafting day 7; the patency rate was 20%, 10%, and 0%, and the average blood flow in the patent TEBV was 1.8, 0.7, and 0 mL/min at postgrafting day 7, 14, and 30, respectively. The CD133 aptamer group had certain TEBV stenosis caused by partial intimal proliferation, a patency rate of 80%, 70%, and 10%, and an average blood flow in the patent TEBV of 5.3, 3.2, and 1.9 mL/min at postgrafting day 7, 14, and 30, respectively. The CD133-ADK chimera group had a patency

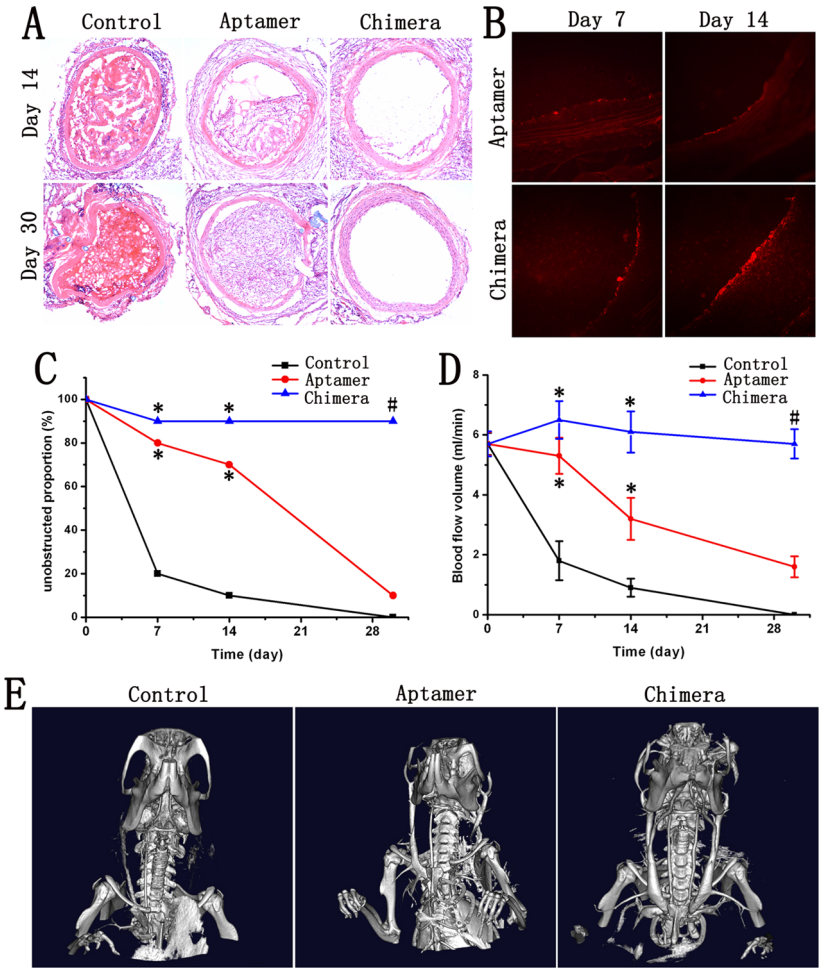

Figure 3. CD133-ADK chimeras upregulated the patency rate of TEBV in diabetic rats. (A) HE staining of TEBVs for 14 days and 30 days. (B) Endothelial cells in cryosections were immunostained for 7 days and 14 days. (C) The unobstructed proportion of TEBV for 7, 14, and 30 days. (D) Blood flow volume of TEBV was determined by Doppler at 7, 14, and 30 days after being transplanted into the rat. (E) Microcomputed tomography angiography at 30 days showed that only CD133-ADK chimera-modified TEBVs remained open, and the arrows indicate the TEBVs. *$p < 0.05$ ($n = 10$) *versus* control TEBV. $^{\#}p < 0.05$ ($n = 10$) *versus* aptamer-modified TEBV. Values are mean ± SD.

rate of 90%, 90%, and 90% and an average blood flow in the patent TEBV of 6.5, 6.1, and 5.7 mL/min at postgrafting day 7, 14, and 30, respectively (Figure 3). Immunofluorescence staining showed that, in the CD133-ADK chimera group, the EC layer was formed in TEBVs at postgrafting day 7 and remained intact at day 14 and day 30. In the CD133 aptamer group, TEBVs were only partially covered by ECs and did not have a complete EC layer at day 14 (Figure 3B, Figure S7). However, HE staining results demonstrated that SMCs had grown through the inner layer of the TEBVs and had grown into the lumen at day 14 (Figure 3A).

CONCLUSIONS

We successfully constructed an aptamer−siRNA chimera-modified TEBV for cell-type-specific capture and delivery. This TEBV reached a patency rate of 90% in diabetic rats 30 days after grafting; mechanistically, CD133 aptamer could selectively capture the CD133-positive cells in the blood; then transfected ADK SiRNA inhibited the apoptosis of CD133-positive cells and promoted the release of adenosine and angiogenesis factors in diabetes mellitus. Our study may provide a new strategy for TEBV construction under disease conditions.

MATERIALS AND METHODS

Cell Culture. Peripheral blood was collected from healthy volunteer donors. Using human lymphocyte separation medium (TBD), we isolated the cloudy mononuclear cell layer by density gradient centrifugation. The cell culture and identification methods were the same as described previously.[9] A magnetic bead separation method was used to isolate CD133-positive cells. After the separation of mononuclear cells, anti-CD133 beads (Miltenyi Biotec) were used for selective sorting, and the sorted cells were cultured as described previously.[9,16] Vascular smooth muscle cells (ATCC) were cultured in DMEM/F12 medium (Hyclone) containing 10% FBS (Gibco).

CD133-ADK Chimeras. CD133-ADK chimeras were designed following the reported methods and comprised two parts: the aptamer and siRNA.[21,22] The CD133 aptamer captures CD133-positive cells and has a sequence of CAGAACGUA UACUAUUCUG.[23] ADK siRNA resists disease damage and has a sequence of GGAGAGAUGACACUAUAAUUU. 2′-OMe modification was used to maintain the stability of chimeras *in vivo*.

Detection of the Ability to Bind CD133-Positive Cells. After 5 days of selective culturing, the cells were trypsinized and incubated with the CD133-PE antibody (Miltenyi Biotec) for 30 min, followed by three phosphate-buffered saline (PBS) washes. Subsequently, 20 nM carboxyfluorescein (FAM)-modified ADK siRNA, CD133 aptamer, or CD133-ADK chimeras were added. After incubation at 37 °C for 15 min and three PBS washes, the samples were subjected to fluorescence detection on a flow cytometer.

Flow Chamber Experiments. After incubation of collagen on a glass slide for 24 h, high-density PEI/PEG-AuNPs were added, followed by 24 h of 1-ethyl-3-(3-(dimethylamino)propyl)-carbodiimide (EDC, Sigma)-induced cross-linking. Next, FAM-modified ADK siRNA, CD133 aptamer, or CD133-ADK chimeras were added and incubated on the slide for 15 min, followed by placement into a flow chamber. In our experiment, we used the maximum shear stress value (30 dyn/cm^2, 1 dyn/cm^2 = 0.1 Pa) measured in the human carotid artery.[24] The width (w) of the flow chamber used in our experiments was 16 mm, and its height (h) was 0.5 mm. The volume flow rate (Q) was 1.54 mL/s, the circulating fluid viscosity (μ) was 1.3 m Pa s, and the wall shear stress was $\tau = 6 \times Q \times \mu/(w \times h^2) = 3$ Pa. The cultured CD133-positive cell suspension at a density of 1×10^5/mL was allowed to flow through the coated slide. Finally, the cells adherent to the slide surface were counted under an inverted microscope.

Synthesis of PEI/PEG-AuNPs. PEG-NHS (Sigma) was slowly added to the PEI (Sigma) in KH_2PO_4/NaOH solution and gently stirred for 48 h. Then the PEI/PEG-AuNPs were synthesized using a one-step method. A total of 1.44 mL of 1% PEI/PEG solution was slowly added into a 14 mM or 42 mM $HAuCl_4$ (Sigma) aqueous solution (25 mL) and stirred at room temperature for 24 h to produce low-density or high-density PEI/PEG-AuNPs, respectively.

Detection of the Ability to Resist Shear Forces. After incubation of collagen on a glass slide for 24 h, PEI or low-density or high-density PEI/PEG-AuNPs were added, followed by 24 h of EDC-induced cross-linking. Next, FAM-modified siRNA was added and incubated on the slide for 15 min, followed by placement into a flow chamber. To simulate the normal shear forces and scouring forces generated by blood flow *in vivo*, the solution in the chamber was driven to flow at a rate of 1.54 mL/s using a circulation pump. After 48 h, the slide was removed and subjected to fluorescence observation under a fluorescence microscope.

Detection of Transfection Capability. FAM-modified siRNA was incubated with Lip2000, PEI, and low-density or high-density PEI/PEG-AuNPs for 15 min and then was added to the SMC culture medium. The cells were cultured at 37 °C for 4 h; after another 24 h of culturing, the cells were subjected to flow cytometry for measurement of average fluorescence intensity.

Construction of PEI/PEG-AuNP-Modified TEBV. Under sterile conditions, 200 g of common carotid arterial tissue was harvested from Wistar rats and rinsed with saline to remove blood. The sample was digested with 0.15% trypsin at 37 °C under 5% CO_2 for 40 min. Nucleic acids and fat in the sample were removed using RNase, DNase, and lipase to obtain vascular matrix material that did not contain any cells and extracellular matrix but had preserved vascular collagen fibers and elastic fibers. Subsequently, the vascular matrix material was incubated with 4 mg/mL of collagen solution for 24 h and was subjected to cross-linking induced by 5 mM EDC (Sigma) for 24 h, followed by three PBS washes. Next, PEI/PEG-AuNPs were added, followed by 5 mM EDC-induced cross-linking for 24 h. Finally, the sample was washed three times with PBS and stored in a 4 °C refrigerator for subsequent use. Before grafting, the TEBV scaffolds were incubated with ADK siRNA, CD133 aptamer, or the CD133-ADK chimera solution for 30 min and then washed three times with PBS. The maximum load and tensile strength of TEBVs were measured using a computer-controlled electronic universal test system.

Animal Experiments. All of the animal experiments were performed in accordance with the regulations on animal experiments of the Third Military Medical University (Chongqing, China) and were approved by the Ethics Committee of the Third Military Medical University. The 8-week-old Wistar rats were intraperitoneally injected with streptozotocin after 12 h of fasting, and the rats with a fasting blood glucose level of >16.7 mmol/L were considered diabetic rats. One month after the successful establishment of diabetic models, the diabetic rats were anesthetized with 1% sodium pentobarbital and underwent TEBV grafting into the right common carotid artery, followed by vascular anastomosis. The blood flow was measured using a Doppler flowmeter at postgrafting day 0, 7, 14, and 30. Furthermore, the grafted TEBVs were removed for frozen sectioning at different time points. A portion of slices was stained with HE staining, and another portion of slices underwent immunofluorescence assays for CD31 (Abcam) and CD133 (Biorbyt). In the immunofluorescence assays, the slices were incubated with the primary antibody at 4 °C overnight, washed three times with PBS, incubated with the fluorescence-conjugated secondary antibody at 37 °C for 1 h, washed three times with PBS again, and finally mounted.

Fluorescence Imaging Detection. TEBVs coated with low-density or high-density PEI/PEG-AuNPs were incubated with the CD133-ADK chimera solution for 30 min and washed three times with PBS. Two days after being grafted into rats, TEBVs were removed and washed to clean up the blood. Finally, the fluorescence intensity was observed using a fluorescence imaging detection system.

Micro-Computed Tomography. One month after TEBV grafting, the diabetic rats were anesthetized with 1% sodium pentobarbital and intraperitoneally injected with 1 mL of heparin. After 5 min of heparinization, the rat's chest was opened to expose the heart for intravascular contrast agent (iopromide) injection. The rats were then sacrificed, and a micro-CT scanner was used to evaluate the patency of the grafts.

Statistical Methods. A t test of the data and the homogeneity of the variance test were performed by using SPSS12.0 software. All of the experimental data were expressed as means ± standard deviation. A p value less than 0.05 was considered a statistically significant difference.

Conflict of Interest: The authors declare no competing financial interest.

Acknowledgment. This work was supported by Training Program of the Major Research Plan of the National Natural Science Foundation of China (No. 91439116), the National Science Foundation of China (No. 31470928), Natural Science Foundation Project of CQ CSTC (cstc2011jjjq0016), the Military Twelfth Five-Year Key Project (BWS11C056), National High Technology Research and Development Program 863 (2012AA020504), and the Research Project of the Ministry of Education and Guangdong Province (2012B091000043).

Supporting Information Available: CD133-ADK chimeras inhibited HG-inducing CD133 positive cell apoptosis (Supplementary Figure 1), CD133-ADK chimeras promoted cell secretion of adenosine and angiogenic factors (Supplementary Figure 2), cell scratch experiment and Transwell migration assay data (Supplementary Figures 3 and 4), CD133-ADK chimeras captured circulating CD133-positive cells *in vivo* (Supplementary Figure 5), characterization of prepared TEBV (Supplementary Figure 6), CD133 aptamer increased TEBV patency rate in rats not induced to be hyperglycemic (Supplementary Figure 7), CD133-ADK chimeras maintained TEBV endothelialization (Supplementary Figure 8). The Supporting Information is available free of charge on the ACS Publications website at DOI: 10.1021/acsnano.5b01203.

REFERENCES AND NOTES

1. Guariguata, L. By the Numbers: New Estimates from the IDF Diabetes Atlas Update for 2012. *Diabetes Res. Clin. Pract.* **2012**, *98*, 524–525.

2. Haraguchi, Y.; Shimizu, T.; Yamato, M.; Okano, T. Concise Review: Cell Therapy and Tissue Engineering for Cardiovascular Disease. *Stem Cells Transl. Med.* **2012**, *1*, 136–141.
3. Dahl, S. L.; Kypson, A. P.; Lawson, J. H.; Blum, J. L.; Strader, J. T.; Li, Y.; Manson, R. J.; Tente, W. E.; DiBernardo, L.; Hensley, M. T.; *et al*. Readily Available Tissue-Engineered Vascular Grafts. *Sci. Transl. Med.* **2011**, *3*, 68ra9.
4. McAllister, T. N.; Maruszewski, M.; Garrido, S. A.; Wystrychowski, W.; Dusserre, N.; Marini, A.; Zagalski, K.; Fiorillo, A.; Avila, H.; Manglano, X.; *et al*. Effectiveness of Haemodialysis Access with an Autologous Tissue-Engineered Vascular Graft: a Multicentre Cohort Study. *Lancet* **2009**, *373*, 1440–1446.
5. Wystrychowski, W.; Cierpka, L.; Zagalski, K.; Garrido, S.; Dusserre, N.; Radochonski, S.; McAllister, T. N.; L'Heureux, N. Case Study: First Implantation of a Frozen, Devitalized Tissue-Engineered Vascular Graft for Urgent Hemodialysis Access. *J. Vasc. Access* **2011**, *12*, 67–70.
6. Dahl, S. L. M.; Blum, J. L.; Niklason, L. E. Bioengineered Vascular Grafts: Can We Make Them Off-the-Shelf? *Trends Cardiovasc. Med.* **2011**, *21*, 83–89.
7. O'Callaghan, T. Options for Off-the-Shelf Blood Vessels Expand. *Nat. News* **2011**, DOI: 10.1038/news.2011.66.
8. Asahara, T.; Murohara, T.; Sullivan, A.; Silver, M.; van der Zee, R.; Li, T.; Witzenbichler, B.; Schatteman, G.; Isner, J. M. Isolation of Putative Progenitor Endothelial Cells for Angiogenesis. *Science* **1997**, *275*, 964–967.
9. Zeng, W.; Wen, C.; Wu, Y. X.; Li, L.; Zhou, Z. H.; Mi, J. H.; Chen, W.; Yang, M. C.; Hou, C. L.; Sun, J. S.; *et al*. The Use of BDNF to Enhance the Patency Rate of Small-Diameter Tissue-Engineered Blood Vessels through Stem Cell Homing Mechanisms. *Biomaterials* **2012**, *33*, 473–484.
10. Rotmans, J. I.; Heyligers, J. M.; Verhagen, H. J.; Velema, E.; Nagtegaal, M. M.; de Kleijn, D. P.; de Groot, F. G.; Stroes, E. S.; Pasterkamp, G. *In Vivo* Cell Seeding with Anti-CD34 Antibodies Successfully Accelerates Endothelialization but Stimulates Intimal Hyperplasia in Porcine Arteriovenous Expanded Polytetrafluoroethylene Grafts. *Circulation* **2005**, *112*, 12–18.
11. Van der Heiden, K.; Gijsen, F. J.; Narracott, A.; Hsiao, S.; Halliday, I.; Gunn, J.; Wentzel, J. J.; Evans, P. C. The Effects of Stenting on Shear Stress: Relevance to Endothelial Injury and Repair. *Cardiovasc. Res.* **2013**, *99*, 269–275.
12. Duckers, H. J.; Silber, S.; de Winter, R.; den Heijer, P.; Rensing, B.; Rau, M.; Mudra, H.; Benit, E.; Verheye, S.; Wijns, W.; *et al*. Circulating Endothelial Progenitor Cells Predict Angiographic and Intravascular Ultrasound Outcome Following Percutaneous Coronary Interventions in the HEALING-II Trial: Evaluation of an Endothelial Progenitor Cell Capturing Stent. *Eurointervention* **2007**, *3*, 67–75.
13. Fredholm, B. B.; AP, I. J.; Jacobson, K. A.; Linden, J.; Muller, C. E. International Union of Basic and Clinical Pharmacology. LXXXI. Nomenclature and Classification of Adenosine Receptors—an Update. *Pharmacol Rev.* **2011**, *63*, 1–34.
14. Shen, H. Y.; Lusardi, T. A.; Williams-Karnesky, R. L.; Lan, J. Q.; Poulsen, D. J.; Boison, D. Adenosine Kinase Determines the Degree of Brain Injury after Ischemic Stroke in Mice. *J. Cereb. Blood Flow Metab.* **2011**, *31*, 1648–1659.
15. Boison, D. Adenosine Kinase: Exploitation for Therapeutic Gain. *Pharmacol. Rev.* **2013**, *65*, 906–943.
16. Chen, W.; Zeng, W.; Wu, Y.; Wen, C.; Li, L.; Liu, G.; Shen, L.; Yang, M.; Tan, J.; Zhu, C. The Construction of Tissue-Engineered Blood Vessels Crosslinked with Adenosine-Loaded Chitosan/beta-Cyclodextrin Nanoparticles Using a Layer-by-Layer Assembly Method. *Adv. Healthc. Mater.* **2014**, *3*, 1776–1781.
17. Barcelos, L. S.; Duplaa, C.; Krankel, N.; Graiani, G.; Invernici, G.; Katare, R.; Siragusa, M.; Meloni, M.; Campesi, I.; Monica, M.; *et al*. Human CD133+ Progenitor Cells Promote the Healing of Diabetic Ischemic Ulcers by Paracrine Stimulation of Angiogenesis and Activation of Wnt Signaling. *Circ. Res.* **2009**, *104*, 1095–1102.
18. Molenaar, C.; Marras, S. A.; Slats, J. C.; Truffert, J. C.; Lemaitre, M.; Raap, A. K.; Dirks, R. W.; Tanke, H. J. Linear 2′ O-Methyl RNA Probes for the Visualization of RNA in Living Cells. *Nucleic Acids Res.* **2001**, *29*, E89–E89.
19. Yin, Y.; Zhao, X.; Fang, Y.; Yu, S.; Zhao, J.; Song, M.; Huang, L. SDF-1alpha Involved in Mobilization and Recruitment of Endothelial Progenitor Cells after Arterial Injury in Mice. *Cardiovasc. Pathol.* **2010**, *19*, 218–227.
20. Sbaa, E.; Dewever, J.; Martinive, P.; Bouzin, C.; Frerart, F.; Balligand, J. L.; Dessy, C.; Feron, O. Caveolin Plays a Central Role in Endothelial Progenitor Cell Mobilization and Homing in SDF-1-Driven Postischemic Vasculogenesis. *Circ. Res.* **2006**, *98*, 1219–1227.
21. McNamara, J. O., 2nd; Andrechek, E. R.; Wang, Y.; Viles, K. D.; Rempel, R. E.; Gilboa, E.; Sullenger, B. A.; Giangrande, P. H. Cell Type-Specific Delivery of SiRNAs with Aptamer-SiRNA Chimeras. *Nat. Biotechnol.* **2006**, *24*, 1005–1015.
22. Dassie, J. P.; Liu, X. Y.; Thomas, G. S.; Whitaker, R. M.; Thiel, K. W.; Stockdale, K. R.; Meyerholz, D. K.; McCaffrey, A. P.; McNamara, J. O., 2nd; Giangrande, P. H. Systemic Administration of Optimized Aptamer-SiRNA Chimeras Promotes Regression of PSMA-Expressing Tumors. *Nat. Biotechnol.* **2009**, *27*, 839–849.
23. Shigdar, S.; Qiao, L.; Zhou, S. F.; Xiang, D.; Wang, T.; Li, Y.; Lim, L. Y.; Kong, L.; Li, L.; Duan, W. RNA Aptamers Targeting Cancer Stem Cell Marker CD133. *Cancer Lett.* **2013**, *330*, 84–95.
24. Fitts, M. K.; Pike, D. B.; Anderson, K.; Shiu, Y. T. Hemodynamic Shear Stress and Endothelial Dysfunction in Hemodialysis Access. *Open Urol. Nephrol. J.* **2014**, *7*, 33–44.